

Extended optical model analyses of $^{11}\text{Be} + ^{197}\text{Au}$ System with dynamic polarization potential

and



Soongsil University
Kyoungsu Heo

Prof. M.K.Cheoun

Prof. K.S.Chi (Korea Aerospace Univ.)

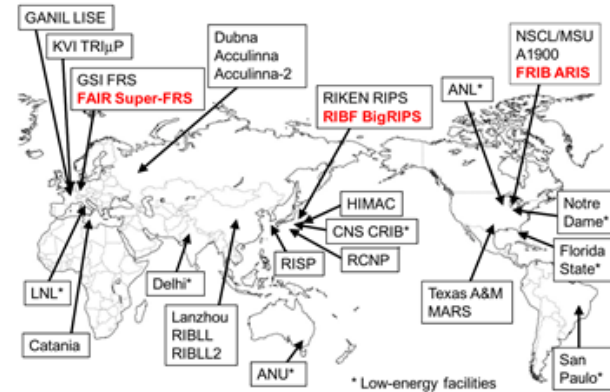
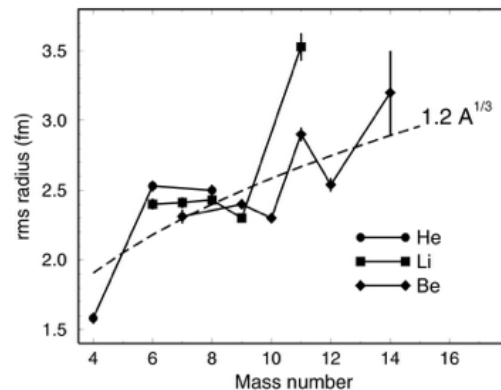
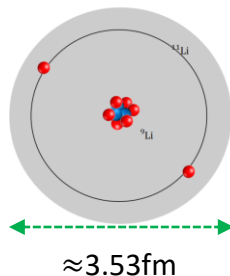
Prof. K.S.Kim (Korea Aerospace Univ.)

Prof. W.Y.So (Kangwon Natl. Univ.)

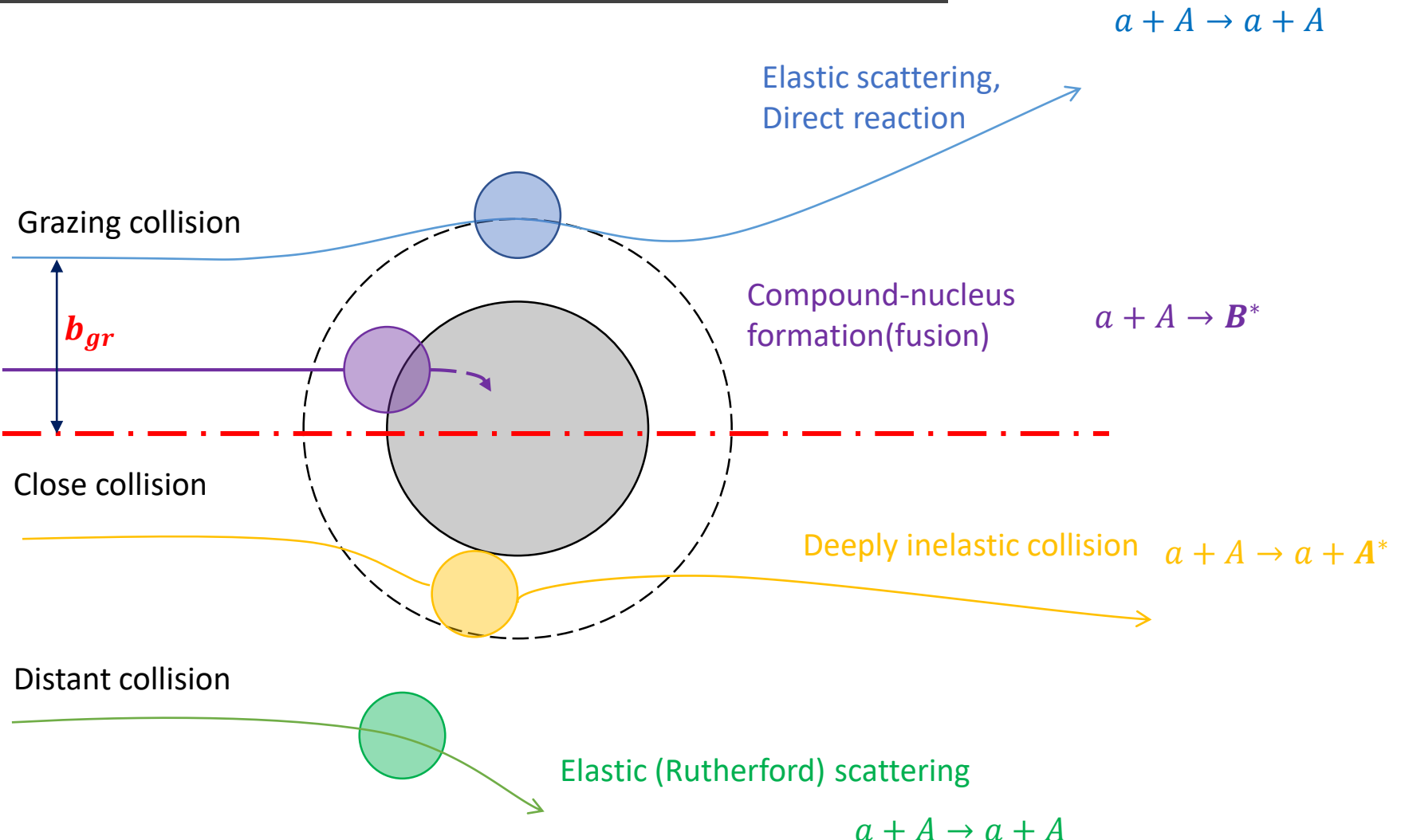
Light Halo Nuclei

Many experiments using **radioactive isotope beams**

- Such as $^{6,8}\text{He}$, $^{19,22}\text{C}$, $^{14,11}\text{Be}$, ^{11}Li
- Become an interesting topic in nuclear physics
- Have several features different from those of stable nuclei
 - They have one or more **valence neutrons**
 - The radii much larger than those of their core
 - **Weakly bound nuclei**
 - Small separation energies
 - The breakup process occurs easily ($a + A \rightarrow b + c + A$)



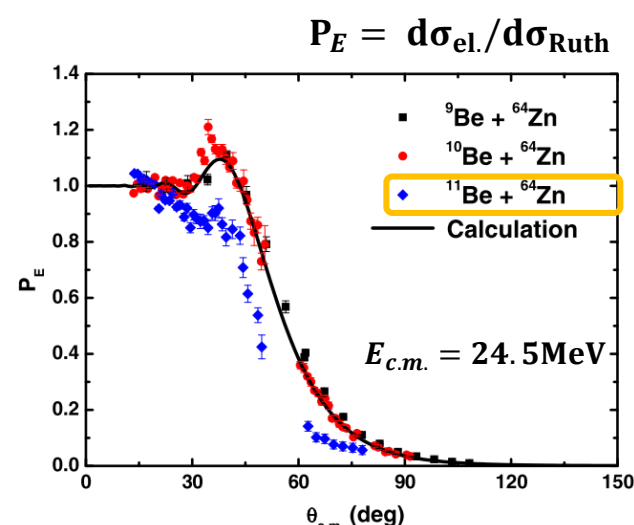
Types of Reactions



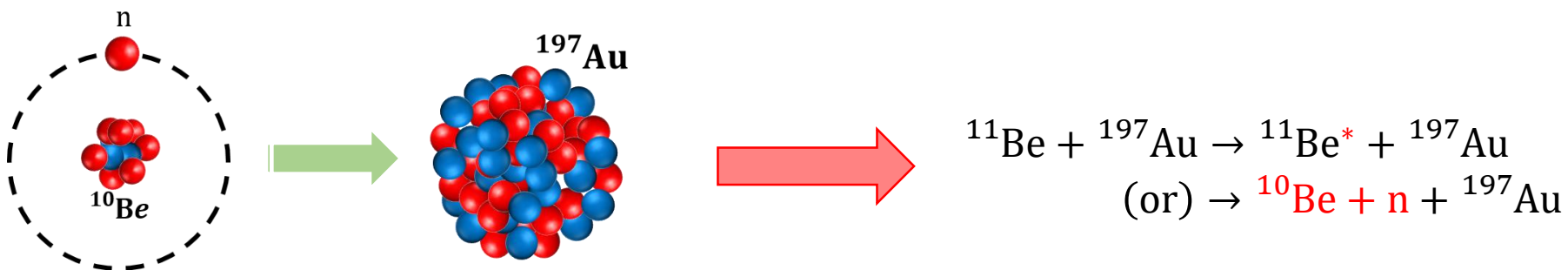
$$* b = \frac{l}{k} = \frac{a_0}{2} \cot \frac{\theta}{2}$$

Coulomb Dipole Excitation Phenomenon

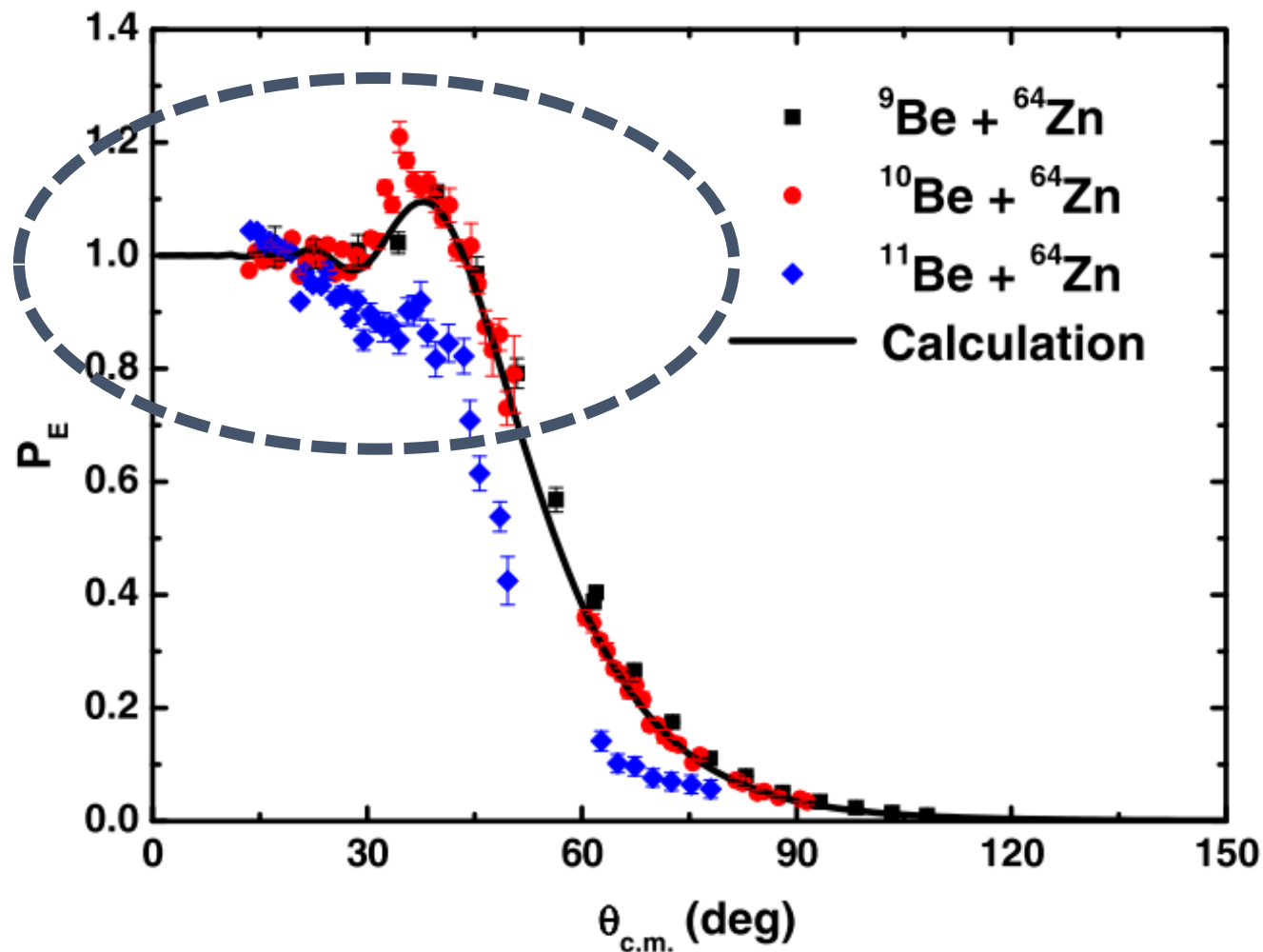
- electric dipole polarization or Coulomb dipole excitation (CDE)
- caused by the **Coulomb repulsive field** generated from the target nuclei
- decelerates the charged nucleus but dose not influence the valence neutron(s)
- The **core nucleus** and **valence neutron(s)** are easily **broken** apart
 - by the effect of **Coulomb field**
- The breakup reaction channels are opened more easily in heavy ion collisions
 - Breakup reaction(or inelastic) cross section↑ ⇒ the elastic cross section↓



W. Y. SO et al.
PRC.92.014627(2015)



Coulomb Dipole Excitation Phenomenon



$$P_E = d\sigma_{\text{el.}} / d\sigma_{\text{Ruth}}$$

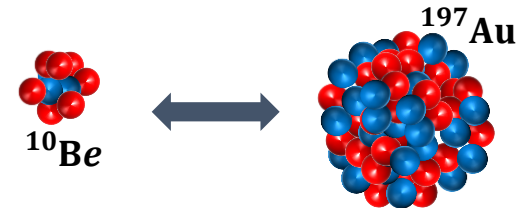
W. Y. SO et al.
PRC.92.014627(2015)

Optical model potential

Complex **optical model** potential (for ^{10}Be)

$$-U_{\text{OM}}^{^{10}\text{Be}} = -U_C(r) + [V_0^{sh}(r) + iW_0^{sh}(r)]$$

$$\begin{aligned} * R_i &= r_i \left(A_T^{\frac{1}{3}} + A_P^{\frac{1}{3}} \right) \\ * r_c &= 1.25 \end{aligned}$$



$$V_0^{sh}(r) = V \left\{ \frac{1}{1 + e^{(r - R_V)/a_V}} \right\}$$

$$W_0^{sh}(r) = W \left\{ \frac{1}{1 + e^{(r - R_W)/a_W}} \right\}$$

$$U_C(r) = \frac{Z_p Z_T e^2}{R_c}$$

$$= \frac{Z_p Z_T e^2}{R_c} \left(\frac{3}{2} - \frac{1}{2} \frac{r^2}{R_c^2} \right)$$

For $r > R_c$

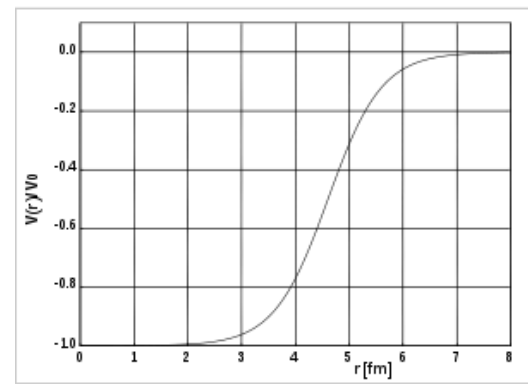
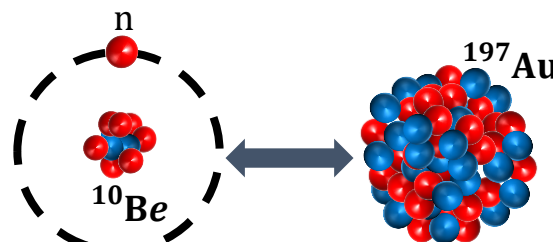
For $r < R_c$

The Extended **optical potential**(for ^{11}Be)

$$-U_{\text{OM}}^{^{11}\text{Be}}(r) = U_{\text{OM}}^{^{10}\text{Be}} + U_0^{lo}$$

$$= U_{\text{OM}}^{^{10}\text{Be}} + \{U_{CDE} + U_{LRN}\}$$

$$= U_{\text{OM}}^{^{10}\text{Be}}(r) + \{U_{CDE}^{br}(r) + U_{CDE}^{inel}(r)\} + U_{LRN}(r)$$



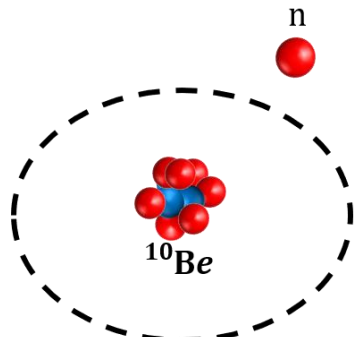
Woods-Saxon potential for $A = 50$, relative to V_0 with $a = 0.5$ fm

https://en.wikipedia.org/wiki/Woods-Saxon_potential

Dynamic Polarization Potential

Coulomb Dipole Excitation Potential

M. V. Andres et al., NPA.579.273-294(1994)



$$\left[\begin{aligned} U_{CDE}^{br}(r) &= V_{CDE}^{br}(r) + iW_{CDE}^{br}(r) \\ &= \frac{4\pi}{9} \frac{Z_t^2 e^2}{\hbar\nu} \frac{1}{(r - a_0)^2 r} \int_{\varepsilon_b}^{\infty} d\varepsilon \frac{dB(E1)}{d\varepsilon} \times \left[g\left(\frac{r}{a_0} - 1, \xi\right) + if\left(\frac{r}{a_0} - 1, \xi\right) \right] \end{aligned} \right]$$

* ε_b is equal to the separation energy $S_n = 0.5$ MeV

* $N = 3.1$ is the proportional constant

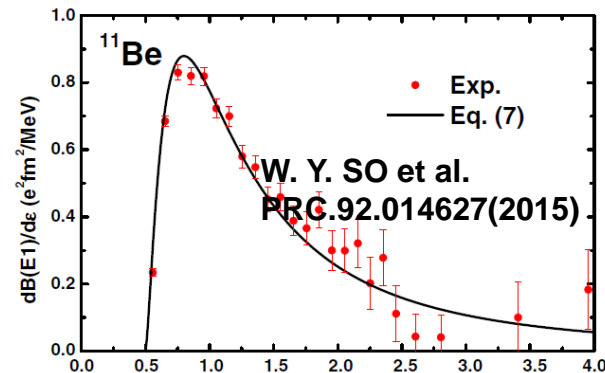
$$\left[\begin{aligned} U_{CDE}^{inel}(r) &= V_{CDE}^{inel}(r) + iW_{CDE}^{inel}(r) \\ &= \frac{4\pi}{9} \frac{Z_t^2 e^2}{\hbar\nu} \frac{B(E1; \varepsilon_x^{1st})}{(r - a_0)^2 r} \times \left[g\left(\frac{r}{a_0} - 1, \xi\right) + if\left(\frac{r}{a_0} - 1, \xi\right) \right] \end{aligned} \right]$$

* $\varepsilon_x^{1st} = 0.32$ MeV

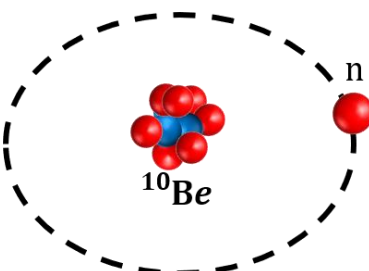
$$* if\left(\frac{r}{a_0} - 1, \xi\right) = 4\xi^2 \left(\frac{r}{a_0} - 1\right)^2 e^{-\pi\xi} K_{2i\xi}'' \left[2\xi \left(\frac{r}{a_0} - 1\right) \right]$$

$$* g\left(\frac{r}{a_0} - 1, \xi\right) = \frac{P}{\pi} \int_{-\infty}^{\infty} \frac{d\xi'}{\xi - \xi'} f\left(\frac{r}{a_0} - 1, \xi'\right)$$

$$* \xi = a_0 \varepsilon / \hbar\nu, \quad a_0 = Z_p Z_t e^2 / 2E_{cm}$$



$$\boxed{\frac{dB(E1)}{d\varepsilon} = N \frac{\sqrt{\varepsilon_b} (\varepsilon - \varepsilon_b)^{3/2}}{\varepsilon^4}}$$



Long Range Nuclear Potential

$$U_0^{lo}(r) = (V_0^{lo} + iW_0^{lo}) 4a_0^{lo} \frac{df(X_0^{lo})}{dr}$$

$$f(X_0^{lo}) = [1 + \exp(X_0^{lo})], \quad X_0^{lo} = \frac{r - R_0^{lo}}{a_0^{lo}} \text{ and } R_0^{lo} = r_0^{lo}(A_1^{\frac{1}{3}} + A_2^{\frac{1}{3}})$$

$E_{\text{c.m.}}$ (MeV) (MeV)	set	V_0^{lo} (MeV)	W_0^{lo} (MeV)	$a_0^{\text{lo}} = a_W^{\text{lo}}$ (fm)	$r_0^{\text{lo}} = r_W^{\text{lo}}$ (fm)	χ^2
37.1	(A)	-0.712	0.0085	5.12	1.5	1.41
	(B)	-0.118	0.0016	5.03	2.5	2.41
	(C)	-0.036	0.0010	4.72	3.5	2.53
29.6	(A)	-0.203	0.0094	7.58	1.5	0.73
	(B)	-0.078	0.0044	7.08	2.5	0.82
	(C)	-0.028	0.0022	6.24	3.5	1.03

$^{11}\text{Be} + ^{197}\text{Au}$ System



PROCEEDINGS
OF SCIENCE

Study of the Scattering of the halo nucleus ^{11}Be on a ^{197}Au target at energies around the Coulomb barrier

M.J.G. Borge[†], V. Pesudo[‡], E. Nácher, O. Tengblad, M. Cubero, A. Perea

Instituto de Estructura de la Materia, CSIC, 28006 Madrid, Spain
mgb@cern.ch

A.M. Moro, J.A. Lay, J. Gómez-Camacho, M.A.G. Alvarez, J.P. Fernández-García

Departamento de FAMN, Universidad de Sevilla, 41080 Sevilla, Spain

A. Di Prieto, P. P. Figuera, M. Fisichella, M. Lattuada, V. Scuderi

Laboratori Nazionali del Sud, INFN, via Santa Sofia 62, 95123, Catania, Italy

V. Pseudo et al. PRL 118, 152502 (2017)

V. Pseudo et al. EPJ Web Conference 163, 00045 (2017)

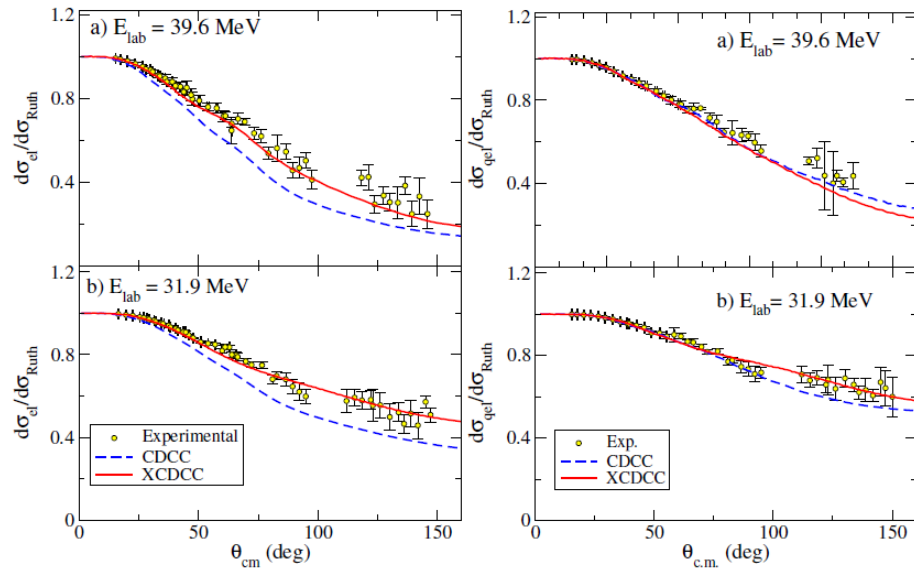
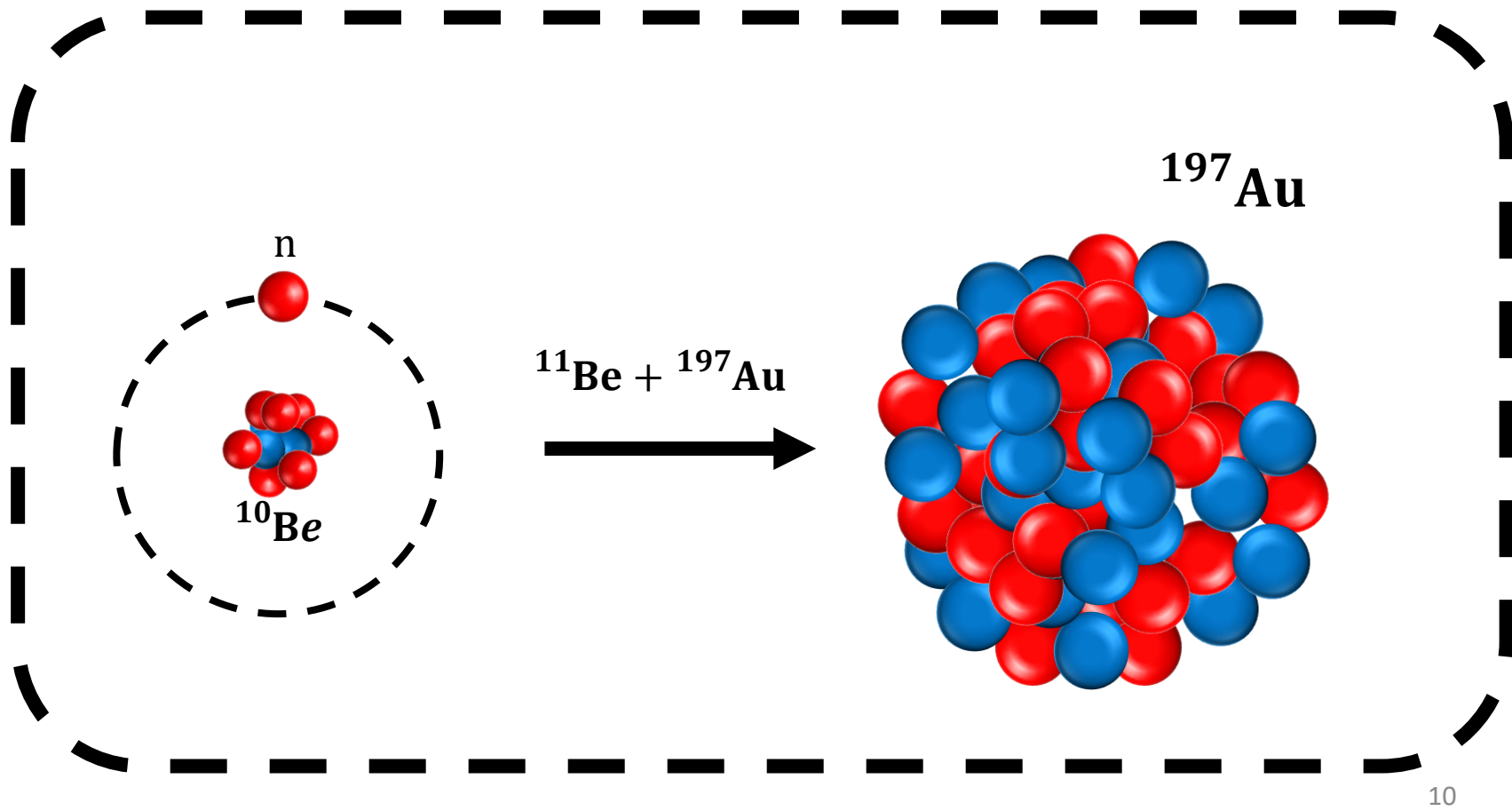


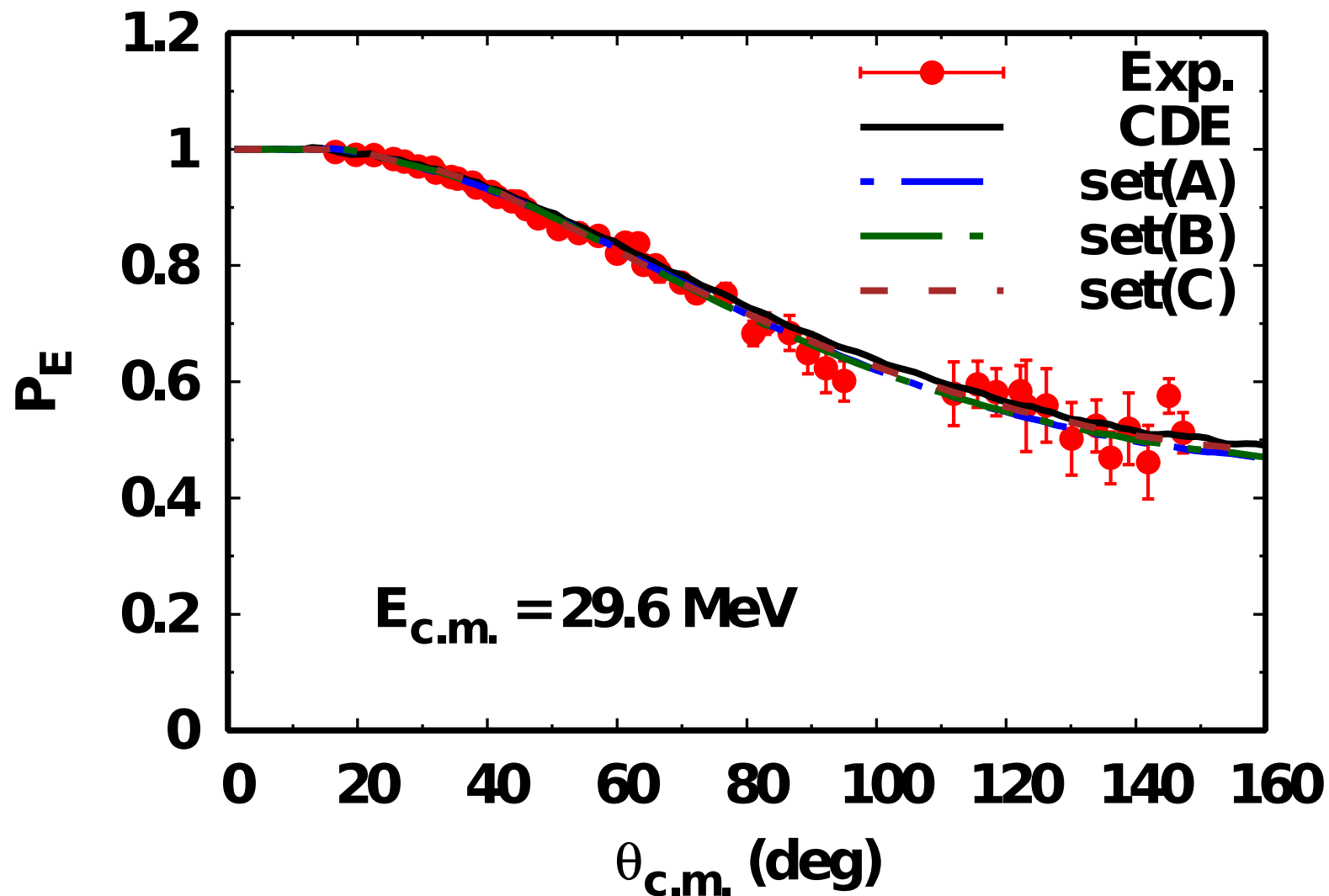
Figure 2: On the left hand side the measured differential elastic scattering cross section of $^{11}\text{Be} + ^{197}\text{Au}$ at $E_{c.m.} = 37.1$ MeV (top) and $E_{c.m.} = 29.6$ MeV (bottom) relative to Rutherford is compared with the CDCC and the XCDCC calculations. There is a significant deviation of the scattering data from the Rutherford formula in the full angular range, even where Coulomb interaction dominates, showing the importance of the dipole polarizability in the collision process. The CDCC calculations underestimate the elastic data since the coupling to the bound excited state in this model is too strong, as discussed in the text. On the right hand side the differential quasielastic cross section relative to Rutherford is shown for $^{11}\text{Be} + ^{197}\text{Au}$ at $E_{c.m.} = 37.1$ MeV (top) and $E_{c.m.} = 29.6$ MeV (bottom). One can see that the CDCC model describes rather well the quasielastic data. XCDCC accounts well for the differential elastic and quasielastic scattering data in the full angular range.

The angular distributions of the **elastic**, **quasi-elastic**, **inelastic** scattering and **break-up** cross section of the one neutron halo ^{11}Be on a heavy mass target (^{197}Au) have been measured at laboratory energies below 31.9MeV and 39.6MeV around the Coulomb barrier($V_b \sim 40\text{MeV}$)

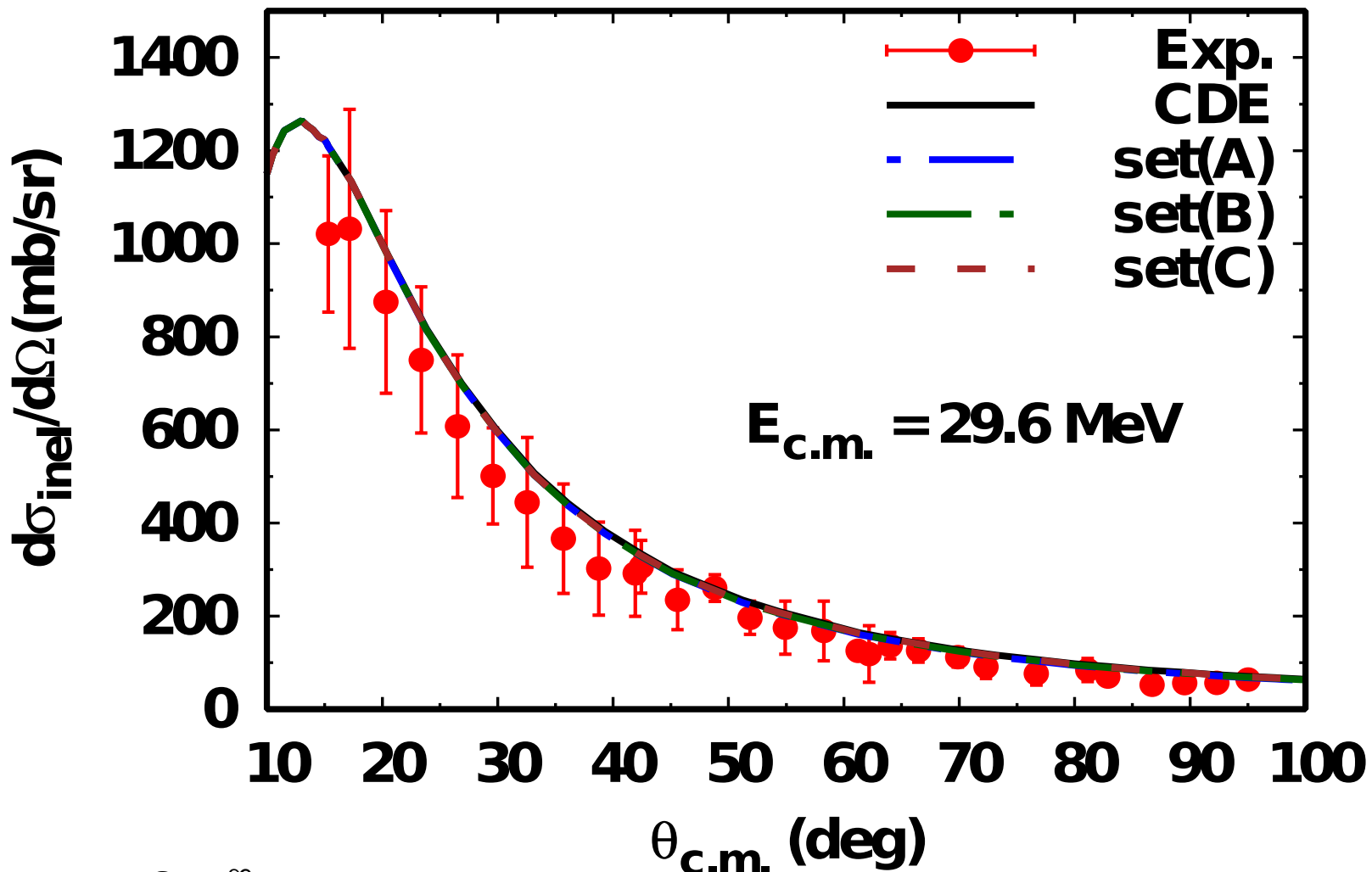
$E_{c.m.} = 29.6 \text{ MeV}$



Elastic Scattering Cross- section in 29.6MeV

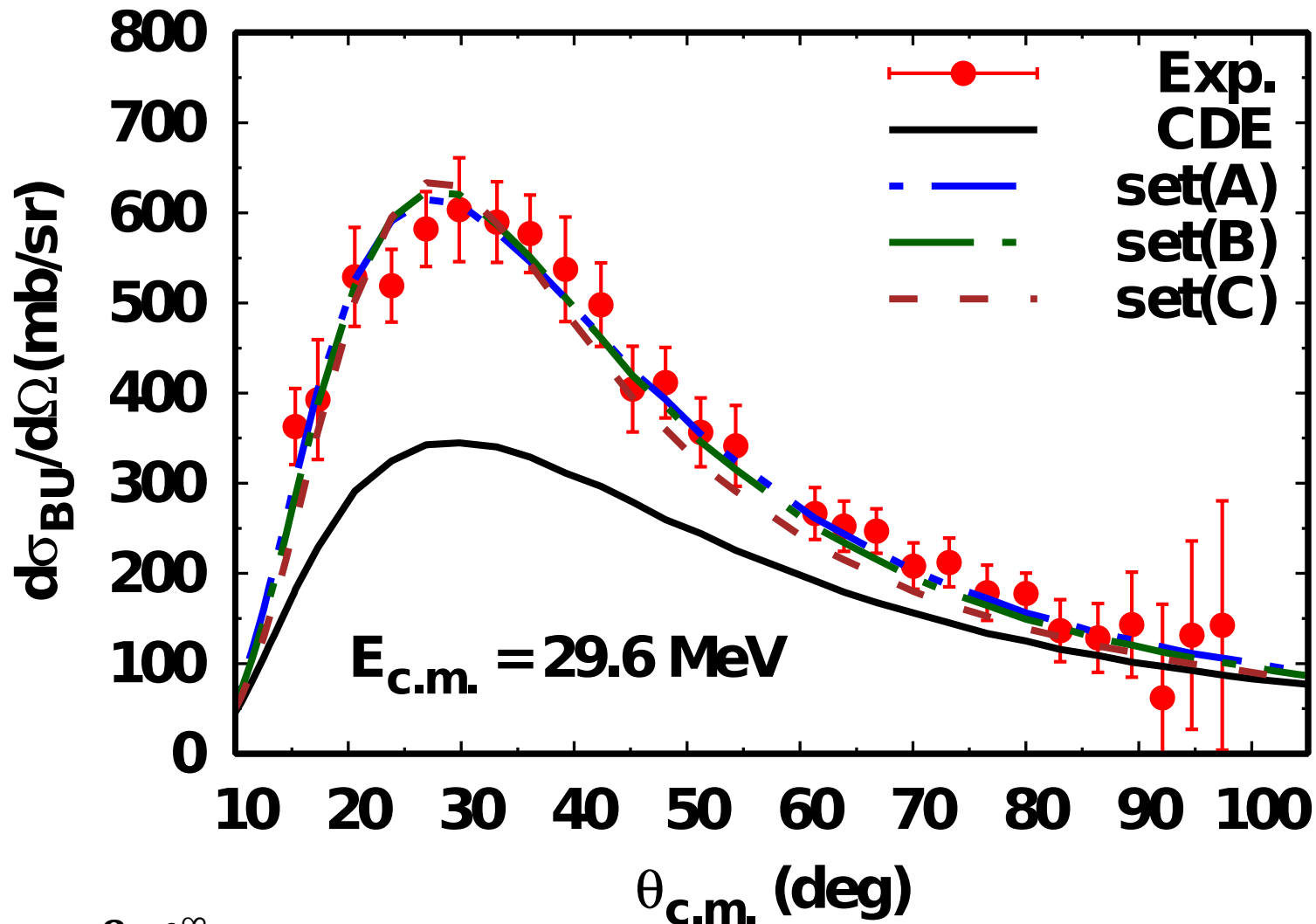


Inelastic Scattering Cross- section in 29.6MeV



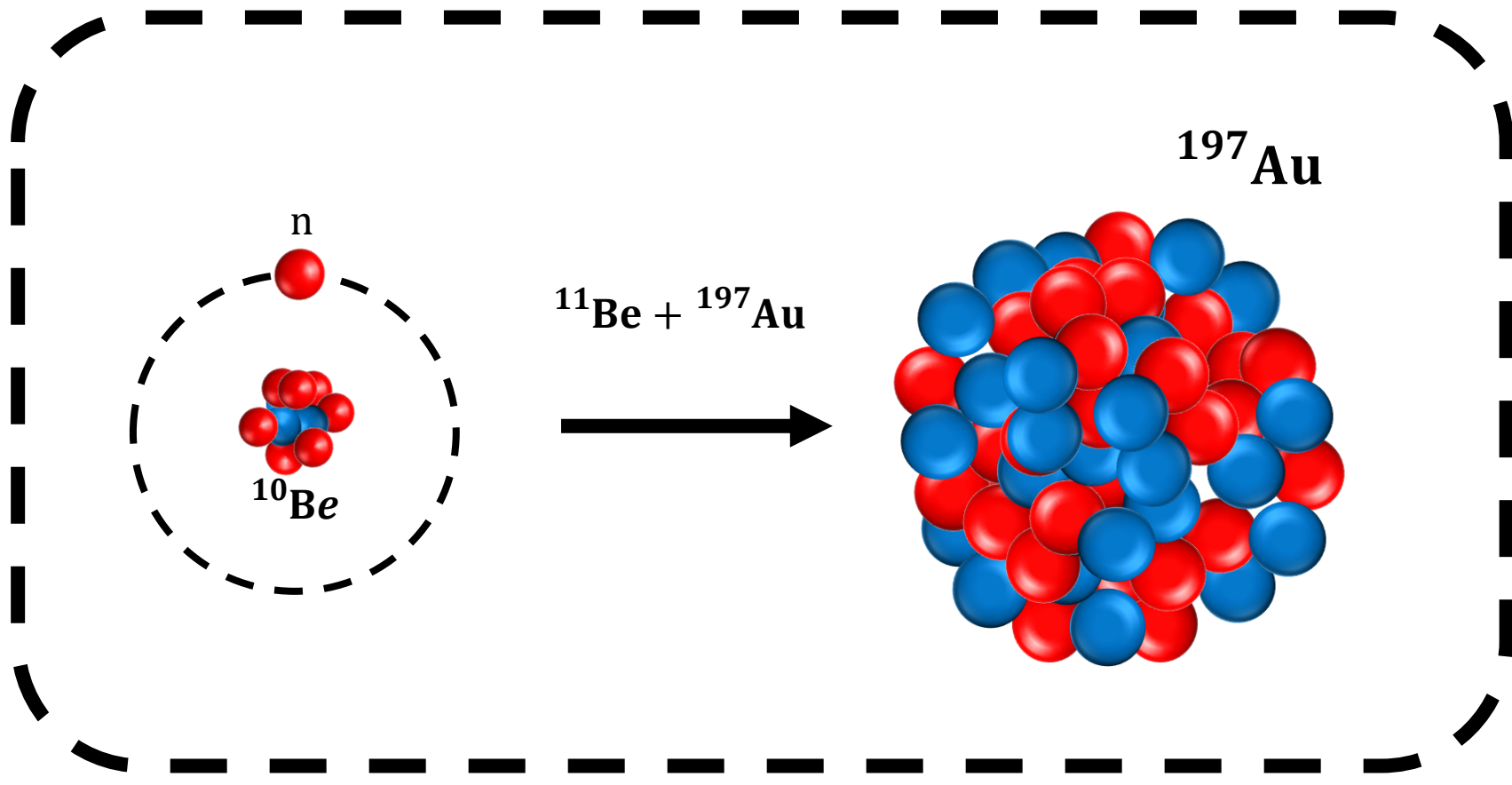
$$T_{inel;l} = \frac{8}{\hbar\nu} \int_0^{\infty} |\chi_l^+(r)|^2 [W_{CDE}^{inel}] dr$$

Breakup Cross- section in 29.6MeV

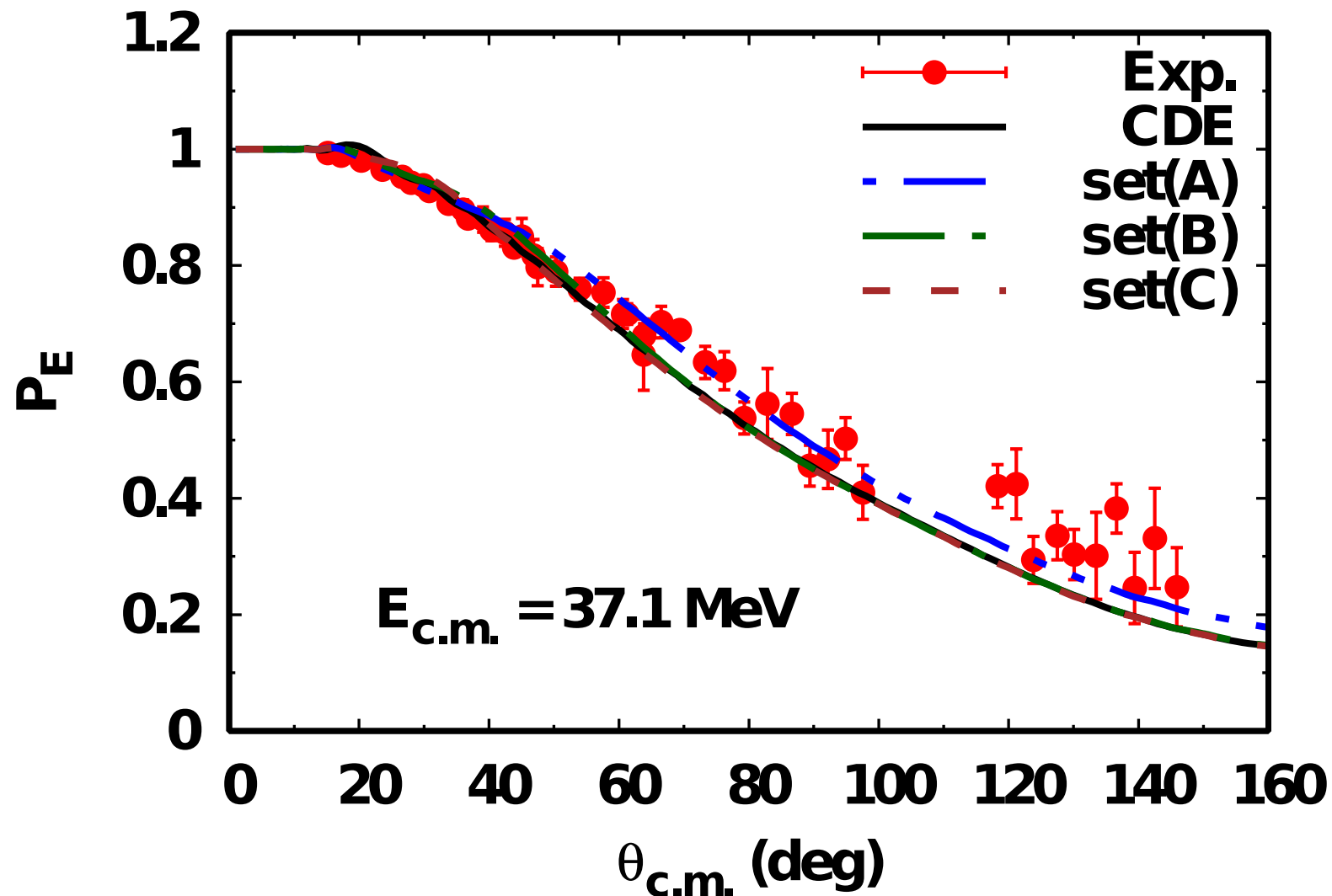


$$T_{BU;l} = \frac{8}{\hbar v} \int_0^{\infty} |\chi_l^+(r)|^2 [W_{CDE}^{br} + W^{lo}] dr$$

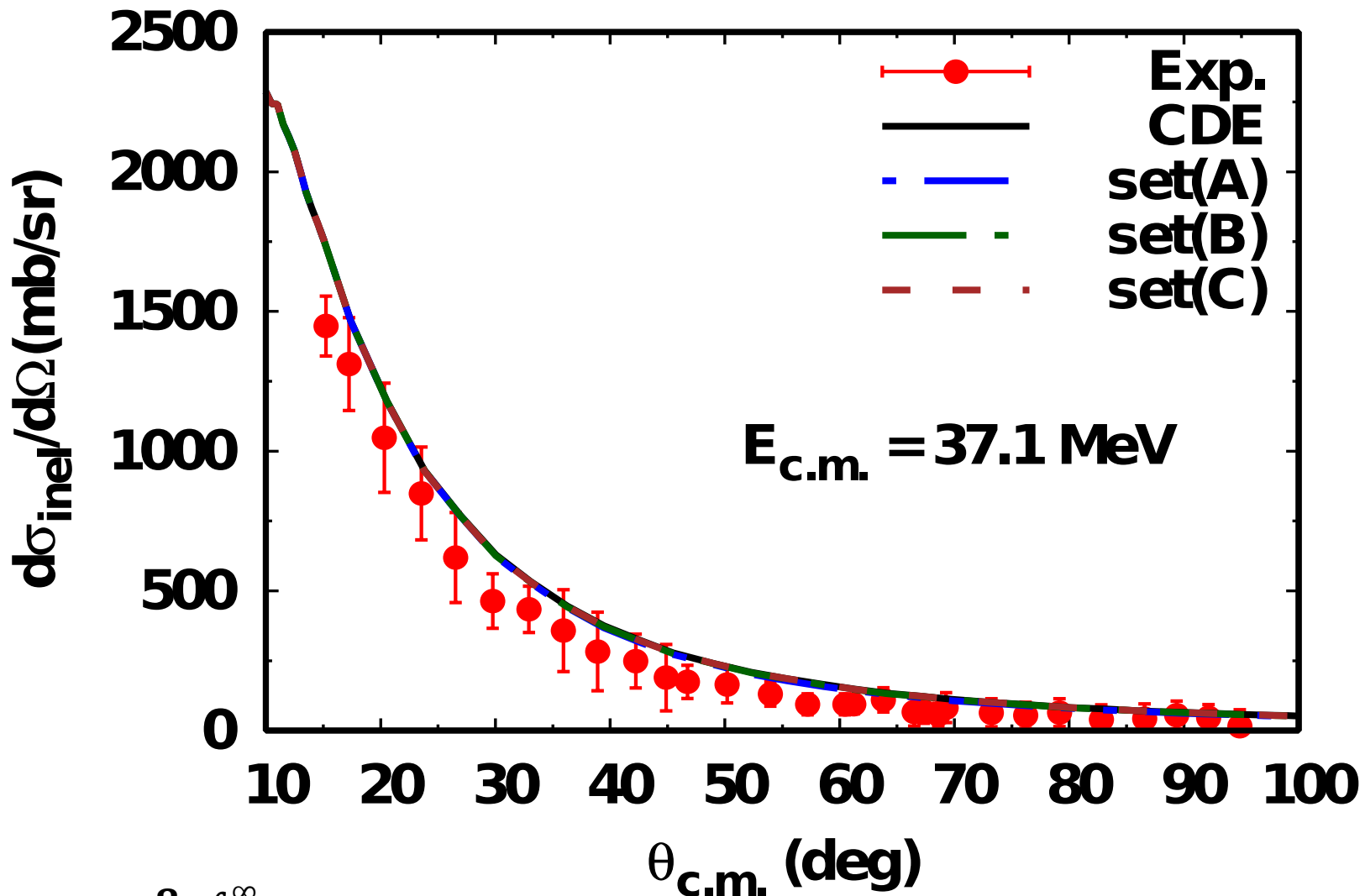
$$E_{c.m.} = 37.1 \text{ MeV}$$



Elastic Scattering Cross- section in 37.1MeV

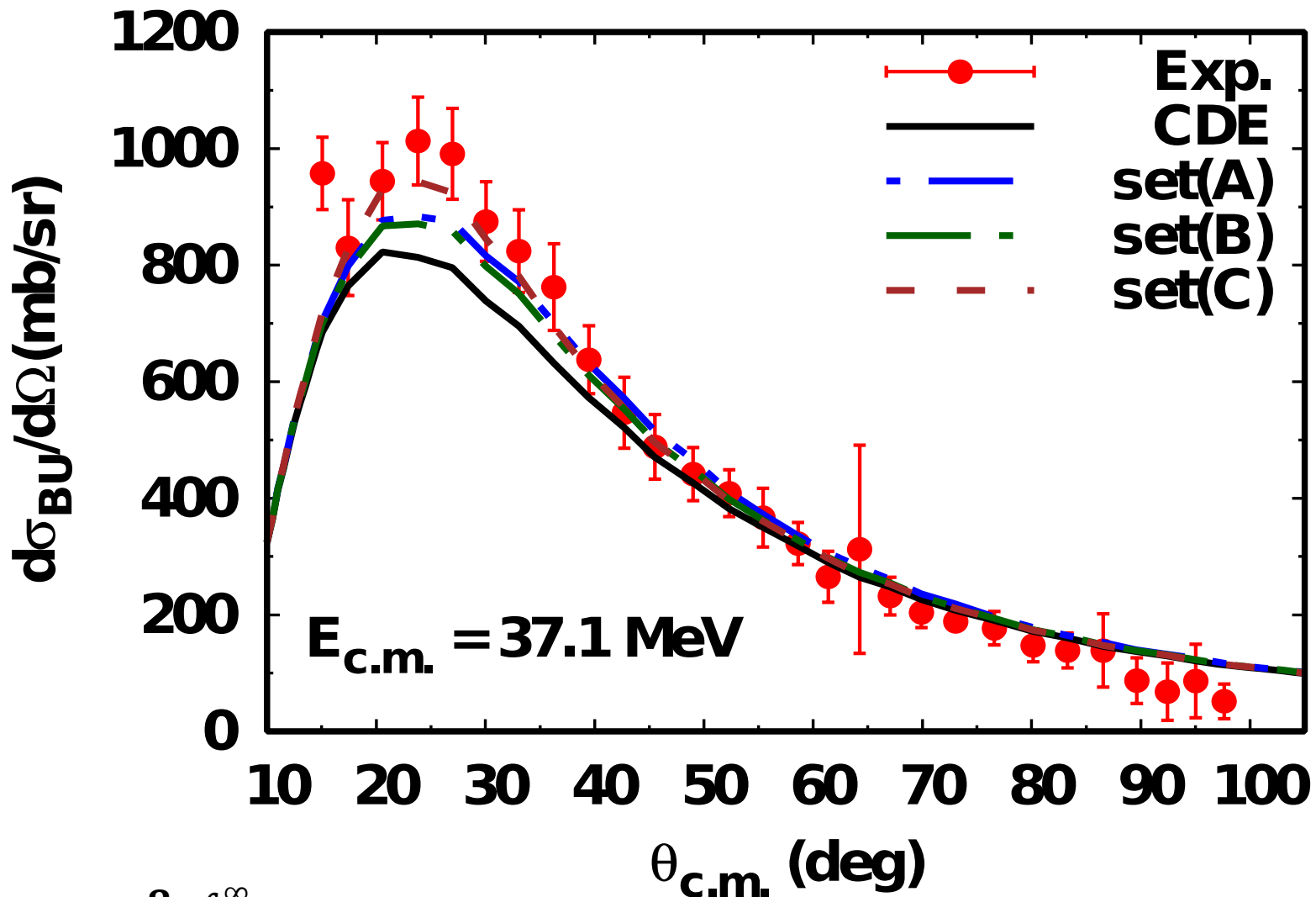


Inelastic Scattering Cross- section in 37.1MeV



$$T_{inel;l} = \frac{8}{\hbar v} \int_0^{\infty} |\chi_l^+(r)|^2 [W_{CDE}^{inel}] dr$$

Breakup Cross- section in 37.1MeV



$$T_{BU;l} = \frac{8}{\hbar v} \int_0^{\infty} |\chi_l^+(r)|^2 [W_{CDE}^{br} + W^{lo}] dr$$

Summary

- We simultaneously calculate elastic, quasi-elastic, inelastic and breakup cross section of $^{11}\text{Be} + ^{197}\text{Au}$ system by taking into account dynamic polarization potential in extended optical model approach.
- Especially, four free parameter for LRN potential by using χ^2 analysis have been used for the all calculations
- We show that the energy dependence of breakup reaction in theoretical frame for checking the influence of CDE potential.

Thank you!!!

$$* \mathbf{S}_L = e^{2i\delta_L} = 1 + 2i\mathbf{T}_L$$

Free: $[E - T]\phi = 0$

$$\hat{G}_0^+ = [E - T]^{-1}$$

Distorted: $[E - T - U_1]\chi = 0$

$$\chi = \phi + \hat{G}_0^+ U_1 \chi$$

Full: $[E - T - U_1 - U_2]\psi = 0$ $\psi = \phi + \hat{G}_0^+(U_1 + U_2)\psi = \chi + \hat{G}_1^+ U_2 \psi$

$$-\frac{\hbar^2 k}{2\mu} \mathbf{T}^{(1+2)} = \langle \phi^{(-)} | (U_1 + U_2) | \psi \rangle$$

$$= \int \phi(U_1 + U_2) \psi dR$$

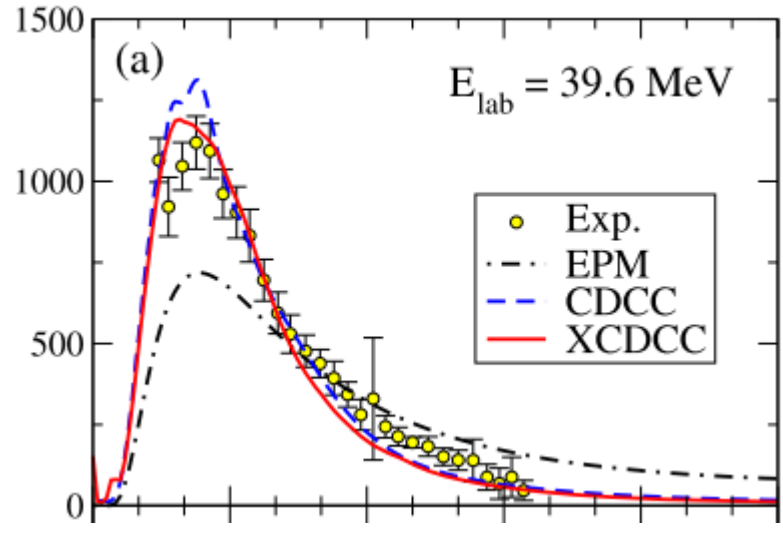
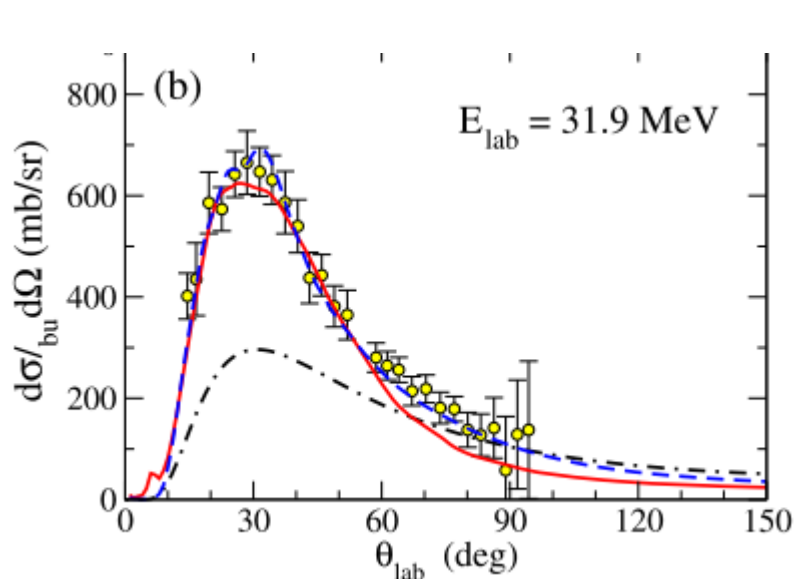
$$= \int (\chi - \hat{G}_0^+ U_1 \chi)(U_1 + U_2) \psi dR$$

$$= \int [\chi(U_1 + U_2) \psi - (\hat{G}_0^+ U_1 \chi)(U_1 + U_2) \psi] dR$$

$$= \int [\chi(U_1 + U_2) \psi - \chi U_1 \hat{G}_0^+(U_1 + U_2) \psi] dR$$

$$= \int [\phi U_1 \chi + \chi U_2 \psi] dR$$

$$= \langle \phi^{(-)} | U_1 | \chi \rangle + \langle \chi^{(-)} | U_2 | \psi \rangle$$



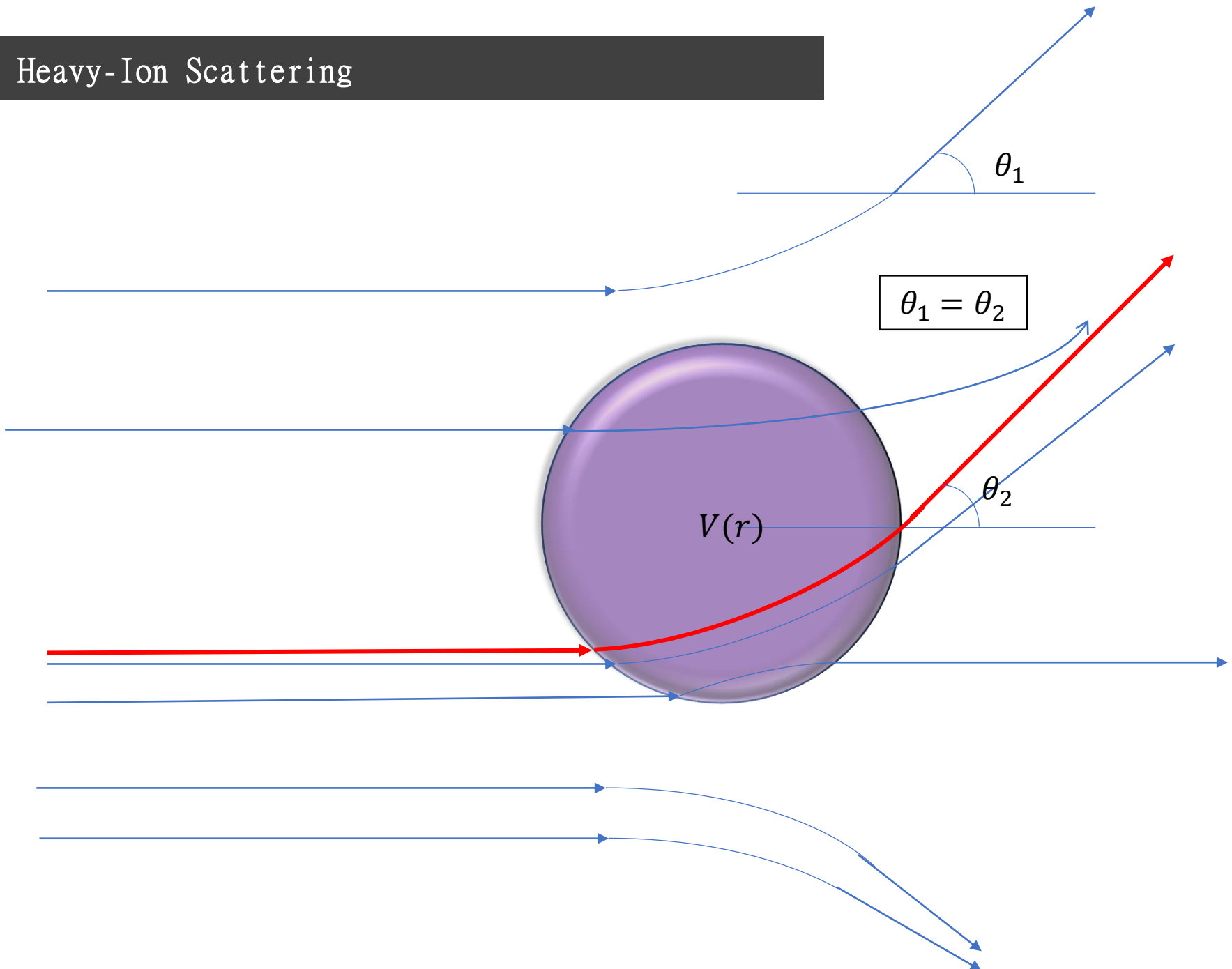
$$\sigma_{lab}(\theta_{lab}, \phi_{lab}) = \frac{(1 + \rho^2 + 2\rho\cos\theta_{c.m.})^{\frac{3}{2}}}{|1 + \rho\cos\theta_{c.m.}|} \sigma_{c.m.}(\theta_{c.m.}, \phi_{c.m.})$$

The **total** angle-integrated cross sections are the same in the lab and c.m. frames (they just measure the total number of incident particles that are deflected by that target)
 However, the **differential** cross sections are different.

In elastic scattering A=C, B=D and Q=0, So we have simply $\rho = m_A/m_B$

$$* \rho = \left[\frac{m_A m_C}{m_B m_D} \frac{E}{Q+E} \right]^{\frac{1}{2}} \quad (\text{B(A,C)D System})$$

Heavy-Ion Scattering



$$P_i \equiv \frac{d\sigma_i}{d\Omega} \Bigg/ \frac{d\sigma_c}{d\Omega} \Bigg(= \frac{d\sigma_i}{d\sigma_c} \Bigg) \quad (i=E \text{ or } D), \quad (1)$$

as a function of the distance of the closest approach D (or the reduced distance d) [1,2] that is related to the scattering angle θ through

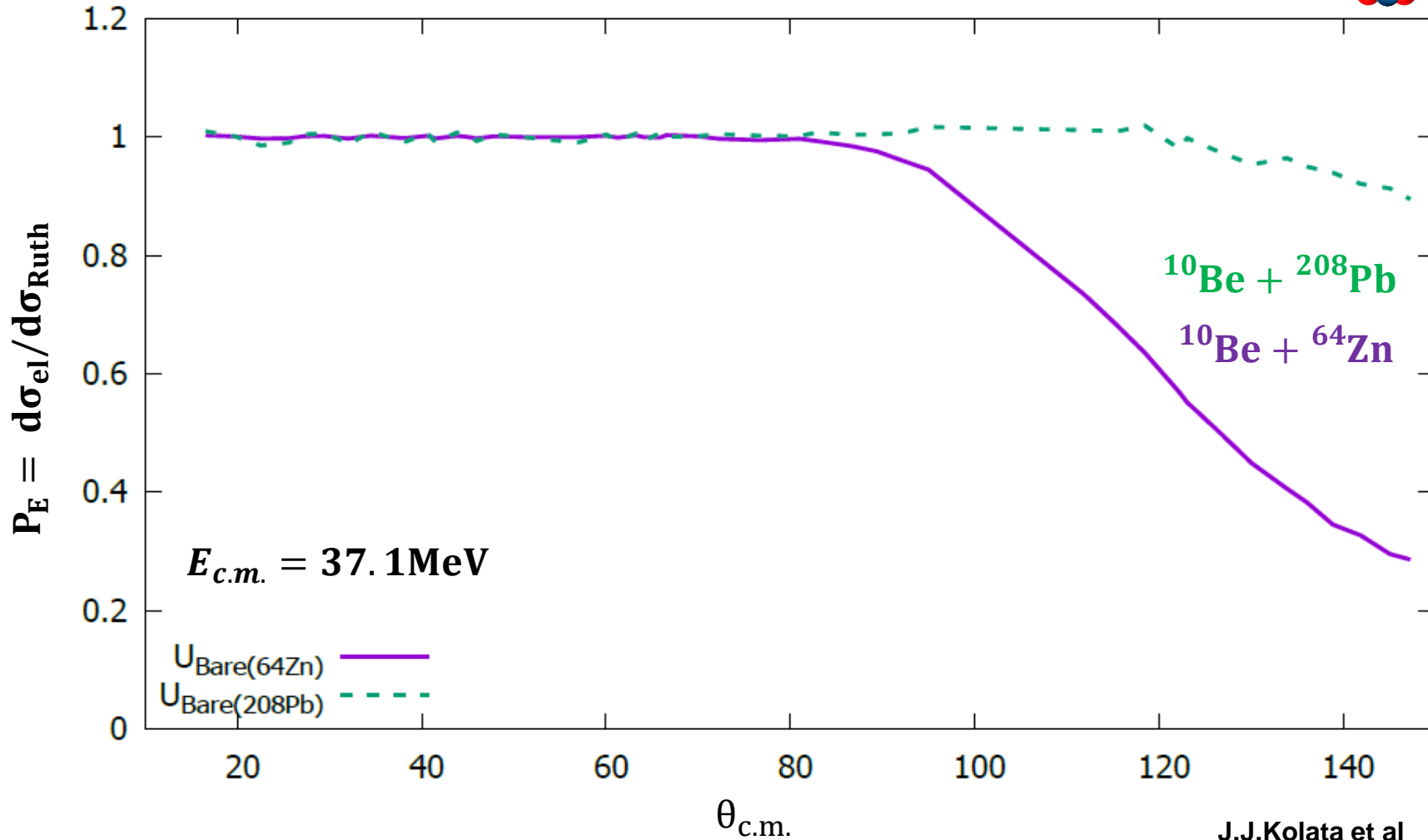
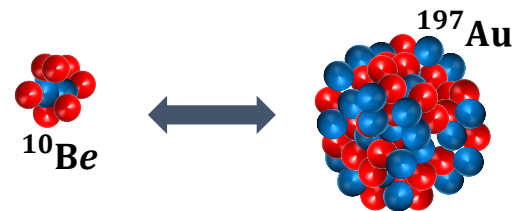
$$D = d(A_1^{1/3} + A_2^{1/3}) = \frac{1}{2} D_0 \left(1 + \frac{1}{\sin(\theta/2)} \right)$$

$$\text{with } D_0 = \frac{Z_1 Z_2 e^2}{E_{\text{c.m.}}}. \quad (2)$$

Here D_0 is the distance of the closest approach in a head-on collision (s wave). Further, (A_1, Z_1) and (A_2, Z_2) are the mass and charge of the projectile and target ions, respectively, and $E_{\text{c.m.}}$ (E_{lab}) is the incident energy in the center-of-mass (laboratory) system. P_E and P_D thus defined may be called the elastic and DR probabilities, respectively. The impact parameter b and orbital angular momentum l , specifying the trajectory, are related to θ and D by

$$b = \frac{l}{k} = \frac{D_0}{2} \cot \frac{\theta}{2} = \sqrt{D(D - D_0)}, \quad (3)$$

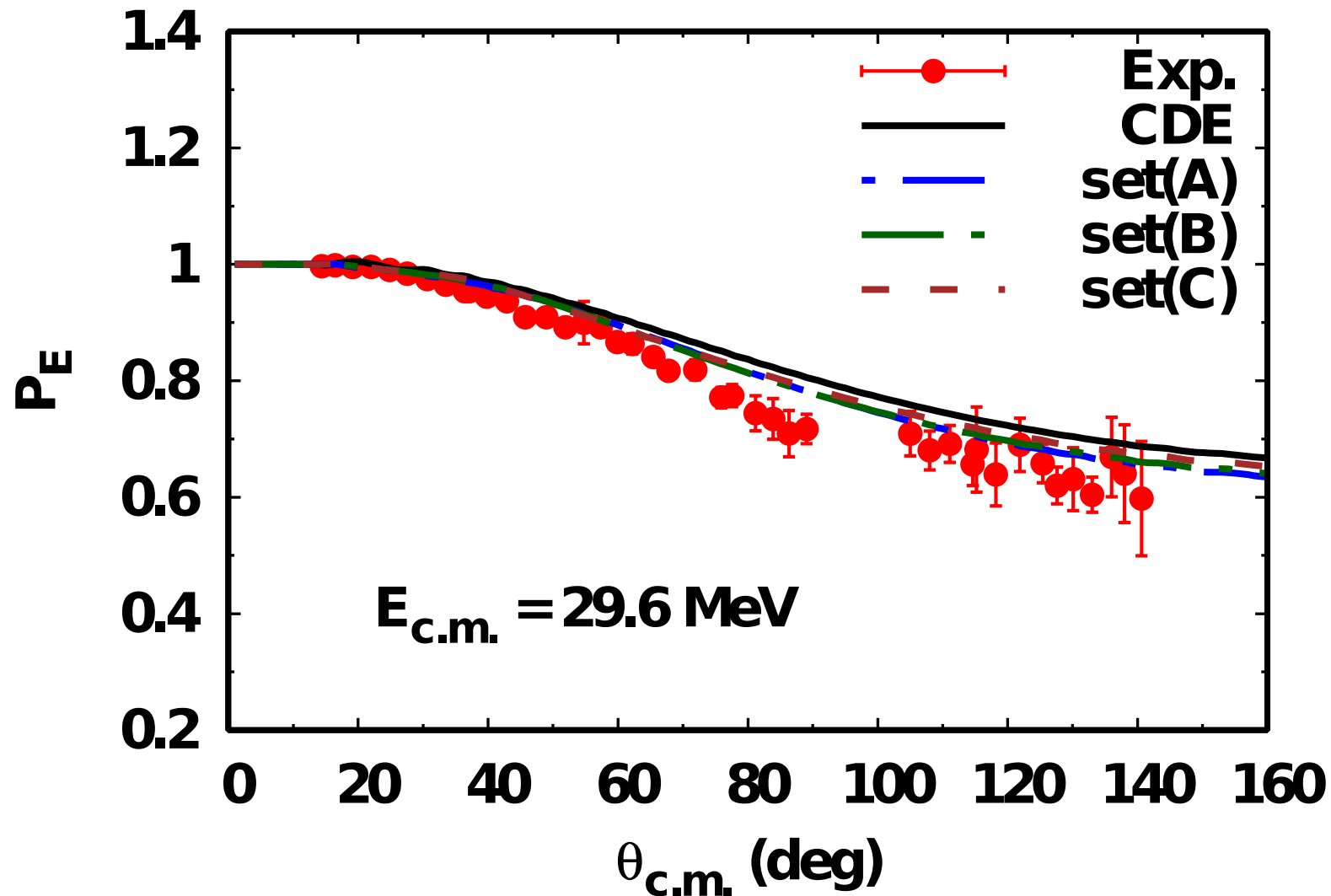
Bare Potentials and Elastic Scattering



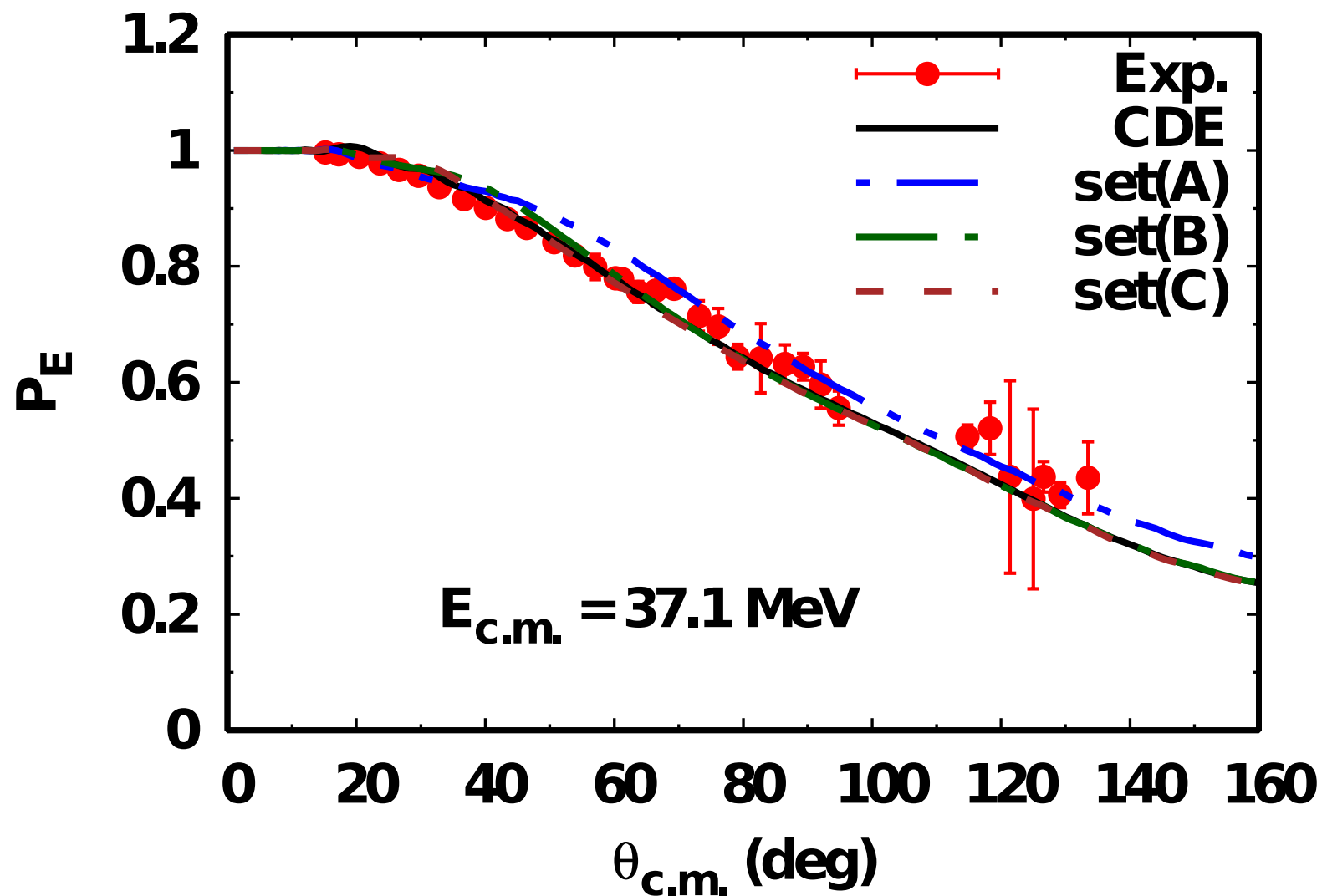
J.J.Kolata et al
PRC.713.(2007),047601

V_0^{sh} (MeV)	W_0^{sh} (MeV)	a_0^{sh} (fm)	a_W^{sh} (fm)	r_0^{sh} (fm)	r_W^{sh} (fm)
113	169	0.63	0.30	1.06	$^{24}_{\text{Au}}$ 1.20)

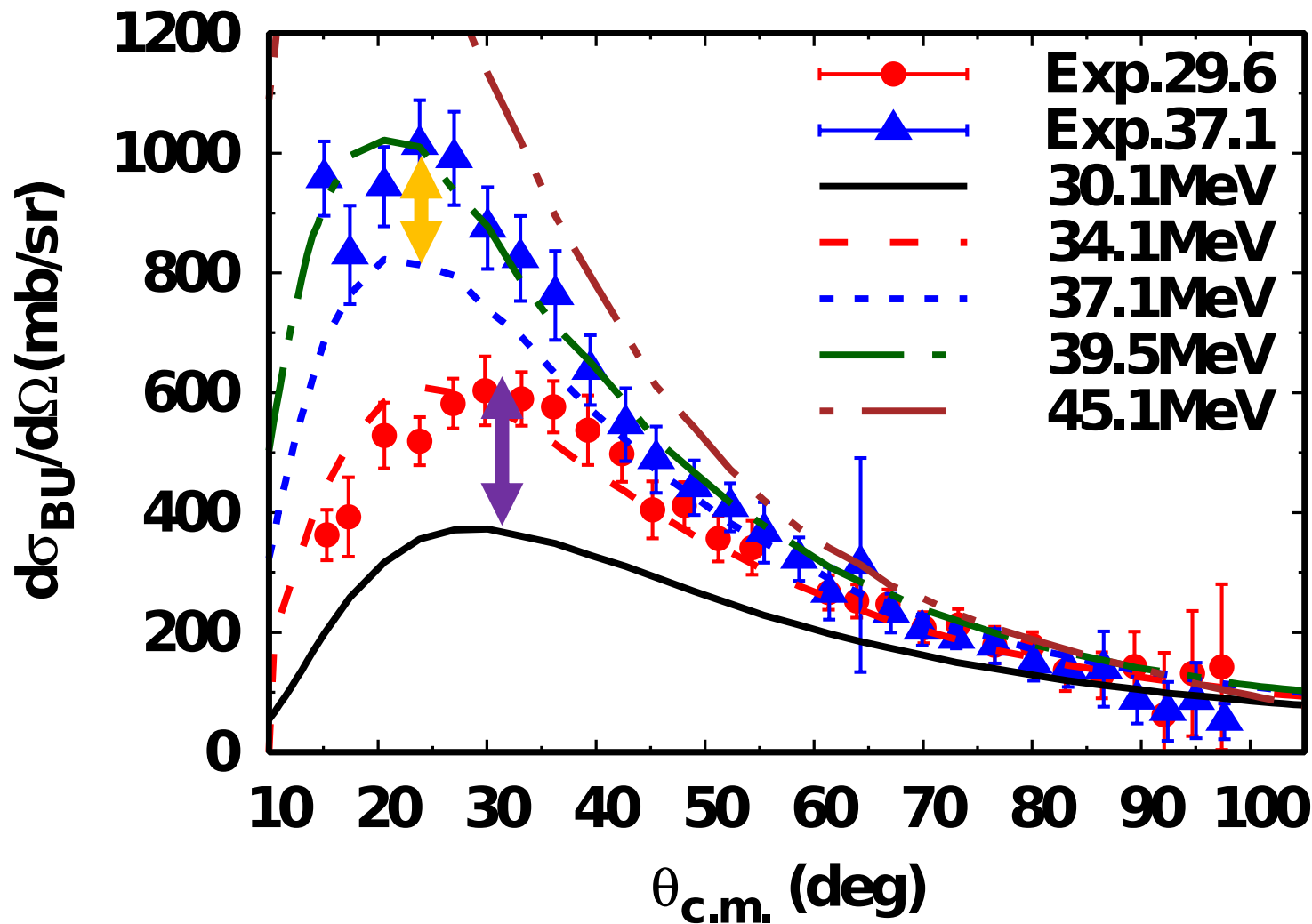
Quasi-elastic Scattering Cross- section in 29.6MeV



Quasi-Elastic Scattering Cross- section in 37.1MeV



Breakup Cross- section in 37.1MeV



$$T_{BU;l} = \frac{8}{\hbar v} \int_0^\infty |\chi_l^+(r)|^2 [W_{CDE}^{br}] dr$$